J Inorg Organomet Polym (2015) 25:687–693
DOI 10.1007/s10904-014-0146-5

Facile Synthesis of Intelligent Polymers Modified Gold Nanoparticles in Aqueous Solution

Cuiping Zhai · Xuejun Liu · Xia Chen · Lina Li · Fang Sun · Huiting Ma

Received: 9 October 2014 / Accepted: 10 December 2014 / Published online: 20 December 2014

Abstract This paper describes the synthesis of gold nanoparticles (GNPs) stabilized with intelligent poly(*N*,*N*-dimethylaminoethyl methacrylate) (PDMAEMA). First, the dithioester-terminated PDMAEMA was prepared by the reversible addition-fragmentation chain transfer technique. Then, the dithioester-terminated PDMAEMA was reduced to a thiol-terminated polymer PDMAEMA-SH. PDMAEMA coated GNPs (Au@PDMAEMA NPs) were synthesized in situ from $HAuCl_4$ aqueous solution by using $NaBH_4$ as a reductant and thiolated PDMAEMA as a stabilizer through Au–S bond. The optical and physical properties of GNPs were characterized by UV–Vis spectroscopy, transmission electron microscopy, X-ray diffraction as well as thermogravimetric analysis. The size and shape of GNPs could be controlled by tuning both the [PDMAEMA]:[$HAuCl_4$] molar ratio and the solution pH. It is believed that these highly biocompatible GNPs have potential biomedical applications.

Keywords Gold nanoparticles · Polymer · Synthesis · Characterization

1 Introduction

In recent years, gold nanoparticles (GNPs) have been the subject of an increasing number of scientific investigations due to their potential applications in the fields of electronics, optics, catalysis and biology [1–5]. In this fascinating branch, functionalized polymers have been widely used as stabilizers, which decorate GNPs via physical or chemical interactions, and the GNPs display unique physical and chemical properties [6–11].

The preparation methods of intelligent polymers modified GNPs mainly include strategies of "grafting from" and "grafting to", and the "grafting-to" approach is especially effective in preparing polymer-stabilized GNPs [12]. Furthermore, polymer-modified GNPs are found to be more stable when the polymer grafts to GNPs through Au–S bond [13–15]. Reversible addition-fragmentation transfer (RAFT) is a well-developed controlled free radical polymerization technique due to its versatility and simplicity. Polymers prepared using this technique carry dithioester end groups, which can be reduced to thiolated polymers by adding reductant (e.g., $NaBH_4$) to the mixtures of $HAuCl_4$ and the dithioester-terminated polymer. Then, GNPs are formed in situ and stabilized by the thiolated polymers via Au–S bond [16].

As a thermo- and pH-sensitive polymer, poly(*N*,*N*-dimethylaminoethyl methacrylate) (PDMAEMA) is widely used in biomedicine materials, such as drug delivery, artificial skin and contact lens [17–19]. Some reports have shown that the GNPs containing PDMAEMA also have thermo- and pH-sensitivity, and have potential applications in the biomedical fields [19–21]. However, the reported results have, up until now, usually focused on the use of copolymer as stabilizing agents, such as PDMAEMA [19, 20] and other polymers. Only Chen et al. [21] have prepared GNPs using single PDMAEMA chains as stabilizing agents. Although their preparation method is very simple, the obtained stable GNP colloid only exists in the case of lower molar ratio of gold to DMAEMA, due to the interaction of DMAEMA and GNPs being weaker than that of other functional groups such as thiols and amine.

C. Zhai · X. Liu (✉) · X. Chen · L. Li · F. Sun · H. Ma
Institute of Fine Chemical and Engineering, Henan University, Kaifeng 475004, Henan, People's Republic of China
e-mail: liuxuejun@henu.edu.cn

C. Zhai
e-mail: zhaicuiping@henu.edu.cn

In this paper, we use a simple route to synthesize GNPs using PDMAEMA chains as stabilizing agents through Au–S bond. The effects of the PDMAEMA concentration and the solution pH on the optical and physical properties of GNPs are also systematically investigated.

2 Experimental

2.1 Materials

N,*N*-dimethylaminoethyl methacrylate (DMAEMA) was obtained from Acros Organics (New Jersey, USA). Azobis(isobutyronitrile) (AIBN) was purchased from Beijing Chemical and Industry Factory and recrystallized before use. *S*-benzyl dithiobenzoate (BTBA) was synthesized and purified according to previous reports [22]. Hydrogen tetrachloroaureate hydrate ($HAuCl_4{\cdot}4H_2O$) and sodium borohydride ($NaBH_4$) were supplied by Sinopharm Chemical Reagent Co., Ltd (Shanghai, China). Other regents were used as received without further purification.

2.2 Sample Preparation

The synthesis protocol for the preparation of PDMAEMA modified GNPs is shown in Scheme 1.

Preparation of PDMAEMA: PDMAEMA was synthesized by a RAFT polymerization using AIBN as an initiator and BTBA as a chain transfer regent. Briefly, DMAEMA (6.44 mL), BTBA (1.31 mL), and AIBN (0.05 g) were dissolved in 22 mL dioxane–water (10:1) mixture and deoxygenated by N_2 bubbling for 30 min. The polymerization was carried out at 80 °C for 36 h and quenched in ice water to stop the polymerization. The product was precipitated in petroleum ether three times and dried at 40 °C in vacuum for 48 h.

Synthesis of Au@PDMAEMA NPs: Thiolated PDMAEMA (PDMAEMA-SH) was prepared as follows: first, 2 mL of 0.5 M $NaBH_4$ aqueous solution was dropped into 10 mL of 5.0 mM dithioester terminated PDMAEMA aqueous solution. The mixture was stirred overnight at room temperature. Then, a given volume of 9.7 mM $HAuCl_4$ aqueous solution was added, and the reaction mixture was stirred for an hour at room temperature. Here, the molar ratio between PDMAEMA and $HAuCl_4$ was adjusted as 1:1, 1:2, 1:3 and 1:4, respectively. For the synthesis of PDMAEMA modified GNPs, a given amount $NaBH_4$ aqueous solution (the molar ratio of $HAuCl_4$/$NaBH_4$ was fixed at 1:3) was added quickly to the vigorously stirred solution. The mixed solution was then stirred in an ice bath for 6 h and the color of the solution turned from yellow to wine-red.

2.3 Characterization

^{1}H NMR spectrum was obtained on a Bruker AV-400 nuclear magnetic resonance (NMR) spectrometer at 400 MHz using D_2O as the solvent. UV–Visible (UV–Vis)

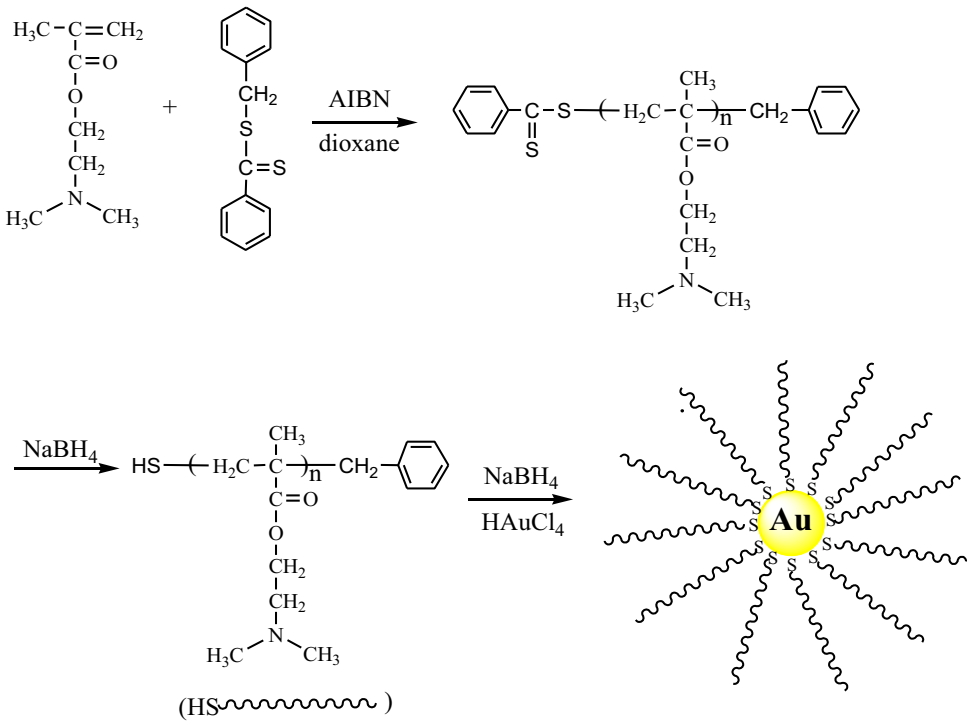

Scheme 1 Synthesis of intelligent polymers modified gold nanoparticles

absorption spectra were obtained on a Thermo Electron UV-5400 spectrometer at room temperature. X-ray diffraction (XRD) was carried out on a Philips X-PertPro X-ray diffractometer. Thermogravimetric analysis (TGA) was carried out under a nitrogen atmosphere using a Mettler Toledo TGA/SDTA851e instrument. TGA measurement was carried out by heating samples from 25 to 800 °C at a heating rate of 10 °C/min. The observed mass loss was attributed to the quantitative degradation of the polymer stabilizer, with the remaining incombustible residues being assumed to be pure gold. Transmission electron microscopes (TEM) were acquired on a JEOL JEM-2010 instrument operating at an acceleration voltage of 80 kV. TEM samples were prepared by dipping a copper grid with

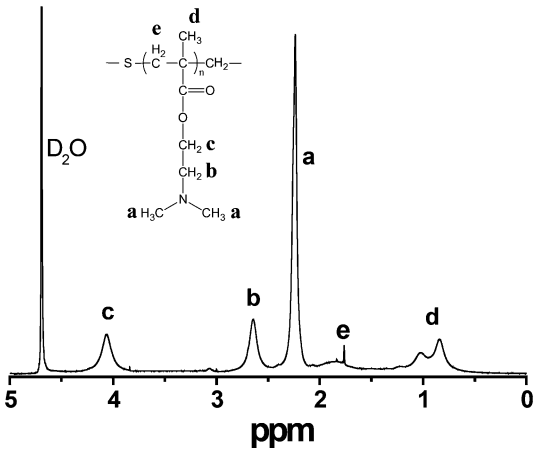

Fig. 1We are very sorry, we found that the molecular structure in Fig.1 is wrong. We changed it, please download in the attachment. ^{1}H NMR spectrum of PDMAEMA in D_2O

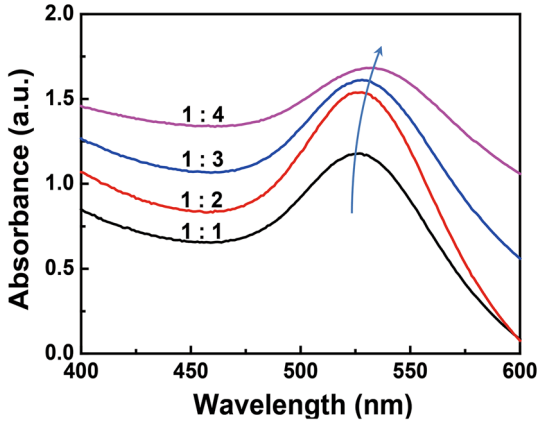

Fig. 3 UV–Vis spectra of gold nanoparticles with different DMAEMA:$HAuCl_4$ molar ratios (1:1, 1:2, 1:3 and 1:4)

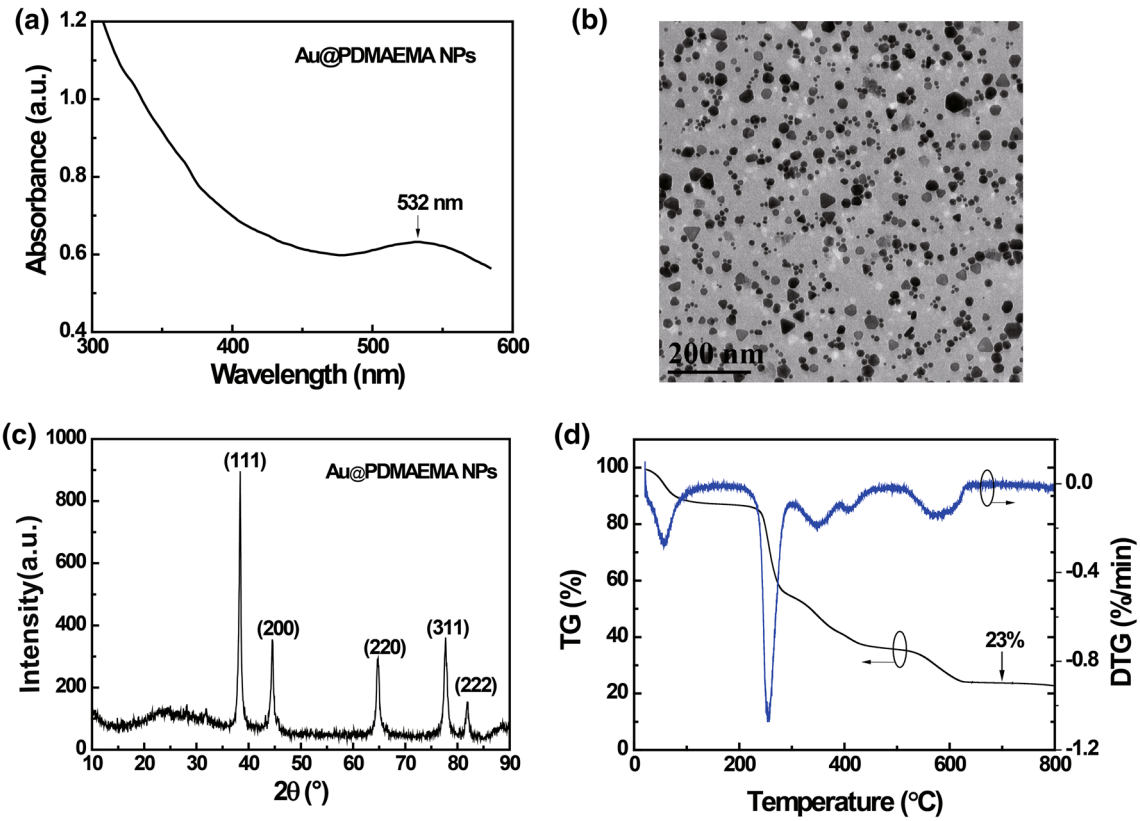

Fig. 2 **a** Absorption spectrum of Au@PDMAEDMA NPs aqueous solution. **b** TEM image of Au@PDMAEDMA NPs. **c** XRD pattern of Au@PDMAEMA NPs. **d** Thermogravimetric (TG) and derivative thermogravimetric (DTG) *curves* of Au@PDMAEMA NPs

carbon film into the prepared gold nanoparicle solution at room temperature.

3 Results and Discussion

The structure of PDMAEMA was investigated by ^{1}H-NMR spectroscopy in D_2O. The ^{1}H NMR spectrum of PDMAEMA is shown in Fig. 1. The resonances at $\delta \sim 0.8$–1.0 ppm and $\delta \sim 1.7$ ppm are assigned to the methyl and methylene protons of backbone (–$\underline{CH_2}C(\underline{CH_3})$–), respectively. The resonance at $\delta \sim 2.2$ ppm is assigned to the methyl protons of –$N(\underline{CH_3})_2$. Furthermore, methylene protons adjacent to nitrogen atom (O–CH_2–$\underline{CH_2}$–N–) and oxygen atom (O–$\underline{CH_2}$–CH_2–N) protons have a resonance appearing around 2.6 and 4.1 ppm, respectively. The results above show that the target polymer PDMAEMA has been synthesized successfully.

Table 1 UV–Vis absorption maxima and diameter distribution of gold nanoparticles with different [DMAEMA]:[$HAuCl_4$] molar ratios and pH

Entry	[DMAEMA]:[$HAuCl_4$]	pH	λ^a_{max} (nm)	Diameter[b] (nm)
NP-1a	1:1	n.d.	525	4.9 ± 1.4
NP-2a	1:2	n.d.	526	9.8 ± 3.9
NP-3a	1:3	n.d.	527	12.2 ± 5.2
NP-4a	1:4	n.d.	532	8.2 ± 2.9
NP-1b	1:1	2.0	531	6.4 ± 1.6
NP-1c	1:1	4.0	532	9.7 ± 2.7
NP-1d	1:1	6.0	533	10.8 ± 3.8
NP-1e	1:1	8.0	535	12.6 ± 4.7

n.d. undetermined

[a] Measured by UV–Vis

[b] Obtained by counting the diameters of 150 nanoparticles from TEM images

With the addition of $NaBH_4$, dithioester terminated PDMAEMA turn into the thiol-terminated PDMAEMA, which can be immobilized on the gold atoms through Au–S bonds. The final solution has a characteristic wine-red color, indicating the formation of colloidal GNPs, in which the [DMAEMA]:[$HAuCl_4$] molar ratios is 1:4. UV–V is absorption spectroscopy shows a broad absorption peak at 532 nm, which is attributed to the surface plasmon resonance (SPR) of GNPs (Fig. 2a) [6, 23]. The morphology of the GNPs was examined using TEM. Under TEM observation, gold has a strong absorbance of electron beam, and Au NPs appear dark. On the contrary, polymer chains around Au NPs have weak absorbance and are not detected [20, 24]. As shown in Fig. 2b, nanoparticles with a wide range of size distribution were obtained, with particle shapes including sphere, rod, plate, and so on.

To gain more insights into the Au@PDMAEMA NPs, powder XRD was used to investigate the crystalline nature of samples (Fig. 2c). Five strong diffraction peaks

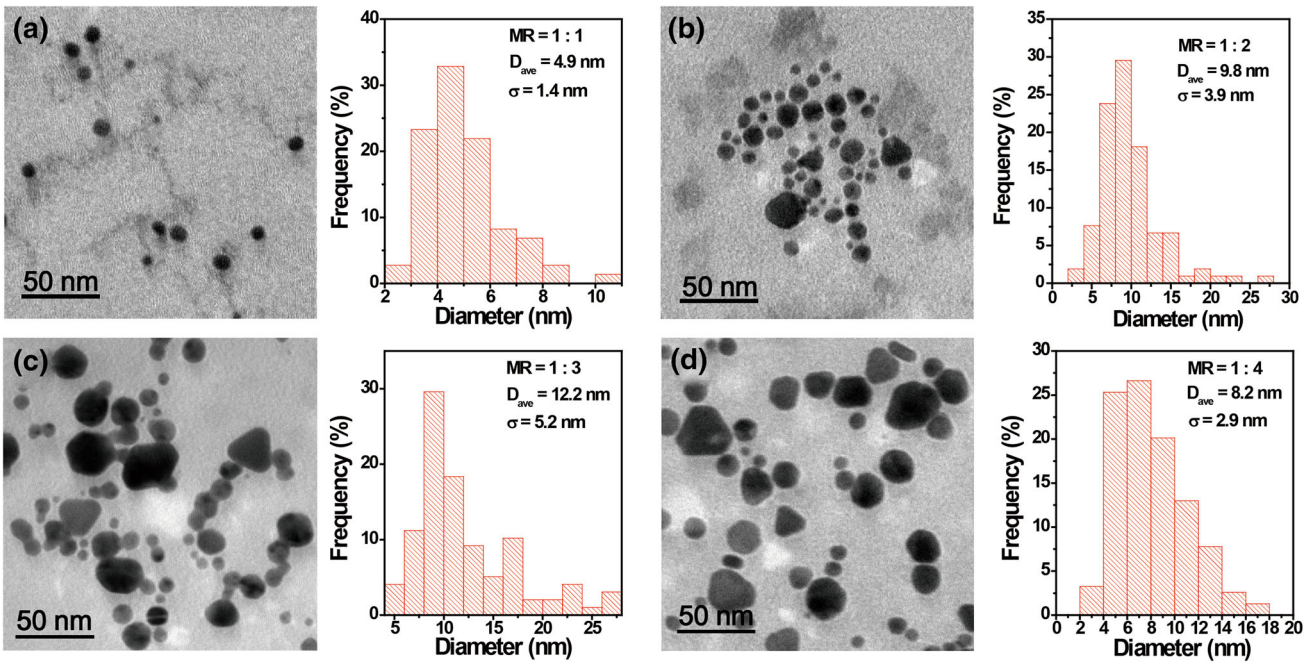

Fig. 4 TEM of GNPs which prepared using different [DMAEMA]:[$HAuCl_4$] molar ratios (**a** 1:1, **b** 1:2, **c** 1:3, **d** 1:4). To the *right* of each micrograph is the size distribution of the corresponding GNPs. In generating the histograms, the diameters of more than 150 NPs were measured for each sample

appearing at 38.3°, 44.5°, 65.0°, 77.7° and 81.9° corresponded to the (111), (200), (220), (311) and (222) planes of a face centered cubic lattice of gold, respectively, and gives direct evidence for the *fcc* structure [25]. Figure 2(d) shows the thermogravimetric (TG) and the derivative thermogravimetric (DTG) curves of the hybrid GNP sample. One can see three stages in the TG curve and this shows that the sample is thermally stable up to 220 °C. After the first stable stage, the TG curve turns down due to decomposition of the organic part starting from 220 to 620 °C. The residual mass shown on TGA analysis reveals that the average polymer content of the GNPs was about 77 % by mass.

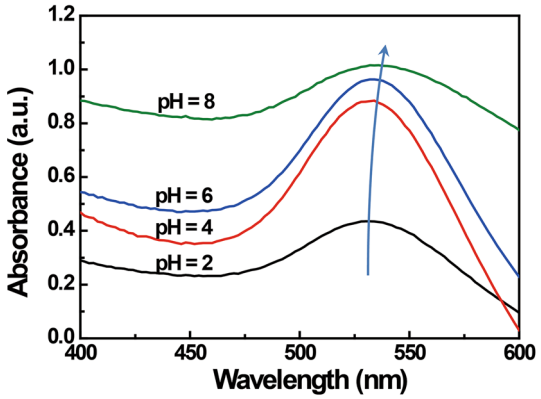

Fig. 5 UV–Vis spectra of Au@PDMAEMA NPs with different pH conditions

A series of Au@PDMAEDMA NPs were prepared at room temperature to examine the effect of the amount of PDMAEMA on GNP size and UV–Vis absorbance. Here, we fixed the concentration of $HAuCl_4$ and varied the amount of PDMAEMA, Au@PDMAEMA NPs with a different [DMAEMA]:[$HAuCl_4$] molar ratio (1:1, 1:2, 1:3 and 1:4.) were prepared. As shown in Fig. 3 and Table 1, with decreasing [DMAEMA]:[$HAuCl_4$], the maximum absorbance wavelength (λ_{max}) of Au@PDMAEMA NPs increased. It is well known that the SPR of GNPs is influenced by the particle size, particle shape and the composition of the polymer [6, 16, 26]. In this experiment, the red shift of SPR band may be due to the increase of nanoparticles size.

To confirm the correlation between the particle structure and the [DMAEMA]:[$HAuCl_4$] molar ratio, the morphology of PDMAEMA-modified GNPs with different [DMAEMA]:[$HAuCl_4$] were investigated by TEM (Fig. 4, the diameter calculation results are listed in Table 1). Figure 4 shows that a different size of nanoparticles are produced by changing the [DMAEMA]:[$HAuCl_4$] molar ratio, and the nanoparticle size is calculated to be 4.9 ± 1.4, 9.8 ± 3.9, 12.2 ± 5.2 and 8.2 ± 2.9 with [DMAEMA]:[$HAuCl_4$] molar ratios of 1:1, 1:2, 1:3 and

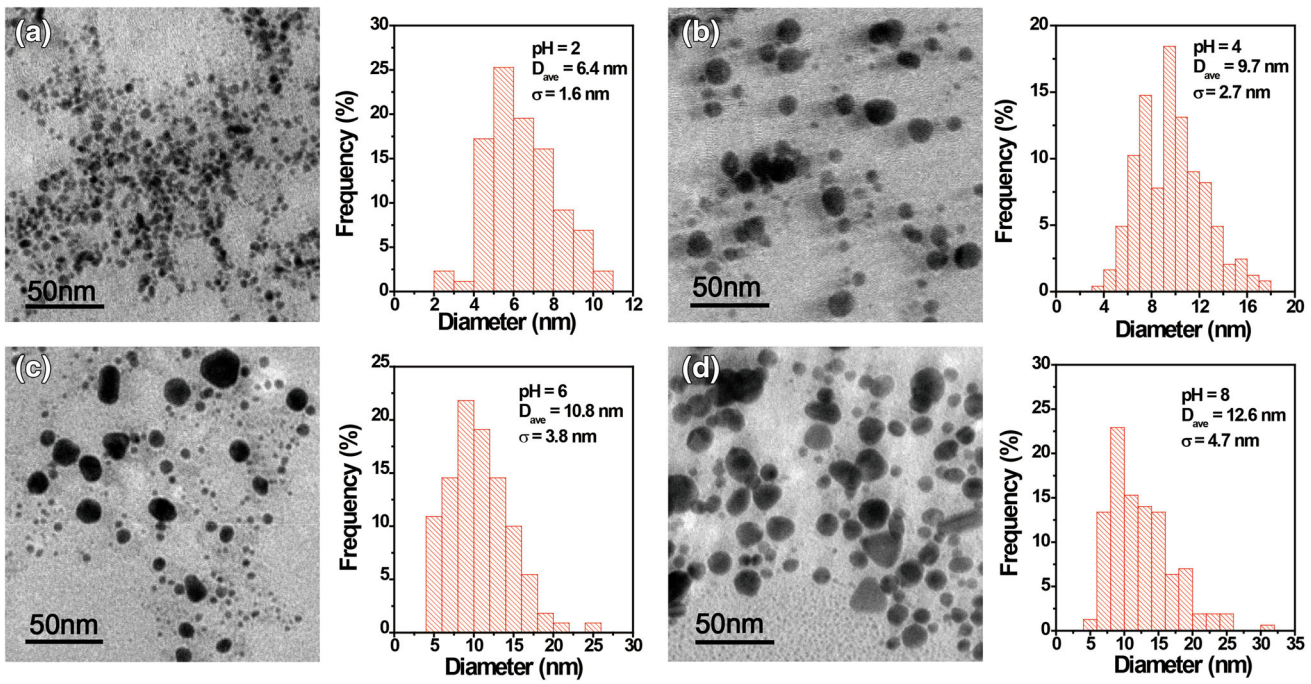

Fig. 6 TEM Figures of Au@PDMAEMA NPs which prepared at different pH values (**a** pH 2, **b** pH 4, **c** pH 6, **d** pH 8). To the *right* of each micrograph is the size distribution of the corresponding GNPs. In generating the histograms, the diameters of more than 150 NPs were measured for each sample

1:4, respectively. It is consistent with the results of UV–Vis spectrum analysis that decreasing [DMAEMA]:[$HAuCl_4$] produces larger nanoparticles. This can be explained by the fact that if the PDMAEMA chain is freely extended in aqueous media, the steric bulk and electrostatic repulsions of the polymer chain can effectively prevent particles from aggregating. Thus, high [DMAEMA]:[$HAuCl_4$] molar ratio results in well-dispersed and smaller NPs (Fig. 4a) [27]. With the decrease in the concentration of the polymer, the amount of polymer around the gold core decreases, and the electrostatic interactions between the gold cores increase, which leads to the nanoparticles tending to aggregate [28]. But, it still contained a large fraction of small particles in the solution (Fig. 4b, c). However, as the concentration of the polymer decreased further ([DMAEMA]:[$HAuCl_4$] = 1:4), the fraction of small particles was reduced (Fig. 4d).

The DMAEMA repeat units have tertiary amines, which can be reversibly protonated by adjusting the pH value. It has been reported that the ionization degree of DMAEMA is 99, 65 and 2 % at pH 5.0, pH 7.0 and pH 9.0, respectively, and altering the pH value has a marked effect on the formation of hybrid NPs [19, 20]. So the pH effect on the size and shape of the Au@PDMAEMA NPs was also studied in this work, and the pH was adjusted by adding HCl and NaOH aqueous solutions to the mixtures. Figure 5 shows the UV–Vis absorption spectra of hybrid NPs with [DMAEMA]:[$HAuCl_4$] of 1:1 at different pH values. It is found that the λ_{max} of NPs dispersion shifts from about 531 nm at pH 2.0–535 nm at pH 8.0 (Table 1), and the absorbance band becomes broader and weaker, suggesting the formation of larger and broader size distributed NPs [29]. It is known that PDMAEMA experienced a transition from extended conformation to a collapsed conformation as the pH of the aqueous system varied [30]. The polymer collapses around gold at higher pH values, which increases the refractive index around gold and induces a red shift of SPR [15].

The morphologies of the Au@PDMAEMA NPs at different pH were also investigated by TEM (Fig. 6). The sizes of the Au@PDMAEMA NPs calculated from the TEM images are 6.4 ± 1.6, 9.7 ± 2.7, 10.8 ± 3.8, and 12.6 ± 4.7 at pH 2.0, 4.0, 6.0, and 8.0, respectively. Such pH-dependent organization of the Au@PDMAEMA NPs could also be explained by the conformational transition of PDMAEMA chains at different pH conditions. When the pH value is 2.0, the polymer chains are freely extended in solution due to strong electrostatic repulsions between the positive charge of protonated PDMAEMA chains, which prevent particles from becoming aggregated [6, 31, 32] (Fig. 6a). So the obtained GNPs have good water dispersibility and much smaller particle sizes. When the pH is adjusted to $\sim$6.0 or even higher, less ionized PDMAEMA chains would collapse onto the surface of the gold cores, which leads to aggregation between NPs [31, 32]. Thus large agglomerates are found when the pH value is higher than 6.0 (Fig. 6c, d).

4 Conclusions

In summary, GNPs coated with stimuli-responsive PDMAEMA polymer were prepared through Au–S bonds. The hybrid GNPs have perfect *fcc* crystalline structure and good thermal stability. The size and shape of the nanoparticles can be controlled by changing the [DMAEMA]:[$HAuCl_4$] molar ratio and the pH value of the aqueous system. The results presented here should shed light on the design and fabrication of nanoscale stimuli-responsive biomaterials.

Acknowledgments Financial support from the Science and Technology Development Program of Henan province of China (132300410235 and 122102210228) is gratefully acknowledged.

References

1. J. Nam, N. Won, H. Jin, H. Chung, S. Kim, J. Am. Chem. Soc. **131**, 13639 (2009)
2. C.M. Cobley, J. Chen, E.C. Cho, L.V. Wang, Y.N. Xia, Chem. Soc. Rev. **40**, 44 (2011)
3. M.C. Daniel, D. Astruc, Chem. Rev. **104**, 293 (2004)
4. R. Sardar, A.M. Funston, P. Mulvaney, Langmuir **25**, 13840 (2009)
5. N. Khlebtsov, L. Dykman, Chem. Soc. Rev. **40**, 1647 (2011)
6. D.X. Li, Q. He, Y. Yang, H. Möhwald, J.B. Li, Macromolecules **41**, 7254 (2008)
7. M. Nuopponen, H. Tenhu, Langmuir **23**, 5352 (2007)
8. H. Guan, W. Wang, X.F. Liu, J.Z. Liang, Colloids Surf. A **448**, 147 (2014)
9. S. Sistach, M. Beija, V. Rahal, A. Brûlet, J.D. Marty, M. Destarac, C. Mingotaud, Chem. Mater. **22**, 3712 (2010)
10. P.W. Zheng, X.W. Jiang, X. Zhang, W.Q. Zhang, L.Q. Shi, Langmuir **22**, 9393 (2006)
11. M.T. Popescu, C. Tsitsilianis, ACS Macro. Lett. **2**, 222 (2013)
12. D.X. Li, Q. He, J.B. Li, Adv. Colloid Interface Sci. **149**, 28 (2009)
13. J. Gao, X.Y. Huang, H. Liu, F. Zan, J.C. Ren, Langmuir **28**, 4464 (2012)
14. I. Blakey, Z. Merican, K.J. Thurecht, Langmuir **29**, 8266 (2013)
15. Y.N. Wen, X.S. Jiang, G.L. Yin, J. Yin, Chem. Commun., 6595 (2009)
16. S.Z. Luo, J. Xu, Y.F. Zhang, S.Y. Liu, C. Wu, J. Phys. Chem. B **109**, 22159 (2005)
17. A.P. Majewski, U. Stahlschmidt, V. Jérôme, R. Freitag, A.H.E. Müller, H. Schmalz, Biomacromolecules **14**, 3081 (2013)
18. X.J. Huang, Y. Xiao, W. Zhang, M.D. Lang, Appl. Surf. Sci. **258**, 2655 (2012)
19. A.E. Smith, X.W. Xu, T.U. Abell, S.E. Kirkland, R.M. Hensarling, C.L. Mccormick, Macromolecules **42**, 2958 (2009)
20. L.Y. Li, W.D. He, W.T. Li, K.R. Zhang, T.T. Pan, Z.L. Ding, B.Y. Zhang, J. Polym. Sci. Part A **48**, 5018 (2010)
21. X. Chen, D.Y. Zhao, L.Z. Zhao, Y.L. Aa, R.J. Ma, L.Q. Shi, Q.J. He, L. Chen, Sci. China Ser. B **52**, 1372 (2009)

22. R.T.A. Maya dunne, E. Rizzardo, J. Chiefari, J. Krstina, G. Moad, A. Postma, S.H. Thang, Macromolecules **33**, 243 (2000)
23. N. Reum, C. Fink-Straube, T. Klein, R.W. Hartmann, C.M. Lehr, M. Schneider, Langmuir **26**, 16901 (2010)
24. H.W. Duan, M. Kuang, D.Y. Wang, D.G. Kurth, H. Möhwald, Angew. Chem. Int. Ed. **44**, 1717 (2005)
25. C.H. Wang, C.J. Liu, C.L. Wang, T.E. Hua, J.M. Obliosca, K.H. Lee, Y. Hwu, C.S. Yang, R.S. Liu, H.M. Lin, J.H. Je, G. Margaritondo, J. Phys. D **41**, 195301 (2008)
26. J.B. Song, L. Cheng, A.P. Liu, J. Yin, M. Kuang, H.W. Duan, J. Am. Chem. Soc. **133**, 10760 (2011)
27. R.G. Shimmin, A.B. Schoch, P.V. Braun, Langmuir **20**, 5613 (2004)
28. S.K. Jewrajka, U. Chatterjee, J. Polym. Sci. Part. A **44**, 1841 (2006)
29. Z.Q. Zhang, Y.H. Wu, Langmuir **26**, 9214 (2010)
30. H. Hu, X.D. Fan, Z.L. Cao, Polymer **46**, 9514 (2005)
31. D.X. Li, Q. He, Y. Cui, J.B. Li, Chem. Mater. **19**, 412 (2007)
32. R. Sardar, N.S. Bjorge, J.S. Shumaker-Parry, Macromolecules **41**, 4347 (2008)